



# Effect of temperature on the structure of Pd<sub>8</sub> and Pd<sub>7</sub>Au<sub>1</sub> clusters: an Ab initio molecular dynamics approach

Analila Luna-Valenzuela<sup>1</sup> · José Luis Cabellos<sup>2</sup> · Alvaro Posada-Amarillas<sup>2</sup>

Received: 31 December 2020 / Accepted: 29 April 2021

© The Author(s), under exclusive licence to Springer-Verlag GmbH Germany, part of Springer Nature 2021

## Abstract

Density functional theory (DFT) is currently one of the most utilized theoretical approaches to analyze physical and chemical properties of metal clusters, which are of interest in economically important applications such as catalysis. In this respect, the important role of temperature has been scarcely considered mainly because this variable is not part of the DFT model and other theoretical ab initio schemes. In this work, we present an ab initio molecular dynamics study of Pd<sub>8</sub> and Pd<sub>7</sub>Au<sub>1</sub> clusters to understand, to a degree, the effect of doping on the structural stability of palladium clusters as a function of temperature. A combined strategy using both empirical potential and DFT calculations is employed to obtain lowest-energy configurations for Pd<sub>8</sub> and Pd<sub>7</sub>Au<sub>1</sub> clusters, which are later subject to Born–Oppenheimer molecular dynamics simulations at finite temperatures. The structural stability as a function of temperature is evaluated through an analysis of the total energy dispersion with respect to the average energy of clusters at different thermodynamic states. Results show that the effect of doping Pd cluster with one Au atom gives rise to a decreasing of the structural stability. In the range of temperatures studied, atomic diffusion is not observed for Pd<sub>8</sub> cluster, while Pd<sub>7</sub>Au<sub>1</sub> cluster shows Pd–Au dimer diffusion at 300 K toward different faces of the 6-atom Pd octahedron structural motif. Preliminary data suggest that melting transition is about 250 K for this bimetallic cluster.

**Keywords** BOMD simulation · Temperature effects · Pd-based clusters · Metal clusters

## 1 Introduction

Mono- and bimetallic nanoparticles exhibit important catalytic activity for a number of relevant technological applications, from catalysis to hydrogen storage devices [1]. This enhanced catalytic activity is basically due to size-related phenomena, such as the confinement quantum effects. In this way, metal nanoparticle properties depend on their size as well as on their shape and composition. Thus, these

properties can be accordingly tuned through the manipulation of the number and type of constituent atoms. Several synthesis methods have been developed to prepare nanomaterials with specific response properties, including chemical, physical, and biological methods [2–4]. This has encouraged the realization of a vast number of investigations focused in the study of small metal nanoparticles or clusters. For example, Heck and Suzuki reactions are catalyzed by palladium clusters [5–10], in which palladium is employed as a catalyst coupling aryl halides with alkenes. Recently, ethylene oxidation studies were conducted utilizing a Cu–Au core–shell nanocatalyst, in which the Langmuir–Hinshelwood mechanism was illustrated through first principles computations [11]. In this work, it is demonstrated that bimetallic clusters display enhanced catalytic properties for ethylene oxide formation. Conversion rate and selectivity have also been analyzed as a function of Pd particle size and morphology. It was found a strong correlation between loading and morphology of the deposited Pd nanoparticles with surfactant type and concentration employed in this work [12].

Published as part of the special collection of articles “20th deMon Developers Workshop”.

✉ Alvaro Posada-Amarillas  
posada@cifus.uson.mx

<sup>1</sup> Programa de Posgrado en Ciencia de Materiales, División de Ingeniería Química Y Metalurgia, Universidad de Sonora, Blvd. Luis Encinas and Rosales, 83000 Hermosillo, Sonora, México

<sup>2</sup> Departamento de Investigación en Física, Universidad de Sonora, Blvd. Luis Encinas and Rosales, 83000 Hermosillo, Sonora, México

The properties of several molecules attached to metal clusters have also been recently investigated [13–15], due to their relevant role in chemical processes to obtain fuels as an alternative to hydrocarbons. Various methods have been implemented in order to obtain methane from biomass, which constitutes a previous step in the process of methanol production through methane oxidation [16]. Several transition metal-based catalysts have been utilized to promote methane oxidation, and recently, a very promising palladium-based catalyst was synthesized, utilizing a zeolite for constraining Pd nanoparticles [17]. This as-prepared catalyst remains active and results to be highly stable and resistant to sintering at realistic temperatures. This is relevant because, besides catalyst poisoning by other atoms or reaction products, temperature modifies the performance of catalysts' activity and selectivity, which is actually a consequence of the change in the respective electronic structure. The effect of other environmental attributes has also been studied, indicating the possible existence of significant effects on the thermodynamic equilibrium state of Au–Pd clusters [18].

Overall, the catalytic properties of nanoparticles are strongly influenced by a number of variables in the preparation method [19], beside those inherent to their elemental composition. From these, temperature remains as one of the most important variables acting upon the catalysts performance, participating in the mechanisms of deactivation and regeneration of catalysts [20]. Despite its fundamental role, this variable is ignored in most of the theoretical approaches utilized to characterize the physical and chemical attributes of metal nanoparticles. Particularly, the density functional theory (DFT) model assumes that temperature is zero, so that the properties at finite temperature remain neglected under this approach. This inability has been replaced by pragmatic exploratory studies of the potential energy surface (PES) employing advanced energy functionals, which are capable of determining several of the different equilibrium configurations, i.e., low-energy isomers [21]. Under this exploratory approach, higher energy isomers are assumed, ad hoc, to possess the structural characteristics of the respective clusters at finite temperature. However, this scheme can be controversial because the analysis of the structural response of metal clusters to temperature should consider thermal effects such as conformational distortions and anharmonic vibrations. In this way, the ideal equilibrium configurations located through theoretical global optimization methods are actually modified by the temperature toward distorted structures, some of which eventually may resemble one of the isomers located in a basin of the PES, but necessarily with consequences on its physico-chemical properties.

In this work, we analyze the structural changes produced by the temperature on the structure and properties of metal clusters utilizing first principles molecular dynamics. We thus compare structures at simulated temperatures with

the ideal structures obtained through global and local PES explorations. DFT reoptimized structures are used as initial configurations in Born–Oppenheimer molecular dynamics (BOMD) canonical (NVT) simulations to examine, under this scheme, the thermal behavior of clusters. The thermodynamical behavior of Pd<sub>8</sub> and Pd<sub>7</sub>Au<sub>1</sub> clusters is analyzed with the simulation data available. The singled-out geometry of the investigated structures corresponds to a bicapped octahedron (bidisphenoid) configuration for both Pd<sub>8</sub> and Pd<sub>7</sub>Au<sub>1</sub> clusters. This cluster size was chosen because it provides a good description of the dynamical behavior of metal clusters at an accurate theoretical representation. Additionally, the lowest-energy configurations of both, the neutral single Au-doped Pd cluster and the pure Pd cluster, are similar irrespective of the theoretical level, as will be shown below. We carried out computations at two theory levels, first utilizing our developed code to perform the empirical global search, and then the deMon2k density functional program [22] for both local optimizations and first principles molecular dynamics simulations.

## 2 Methodology

### 2.1 Theoretical Approaches

An extensive global search of the lowest-energy configurations at the empirical level of theory for Pd<sub>8</sub> and Pd<sub>7</sub>Au<sub>1</sub> clusters was carried out employing our locally developed Basin-Hopping University of Sonora (BHUoS) code [23]. In this program, the basin-hopping method [24] is implemented to explore the Gupta potential hypersurface for mono- and bimetallic clusters. The semiempirical many-body Gupta potential is derived for metal systems within the tight-binding second-moment approximation and has been successfully used to model diverse condensed phase systems [25–27]. For further details, the reader is referred to the work by Cleri and Rosato [28]. The average Gupta potential parameters describing homogeneous (Pd–Pd and Au–Au) and heterogeneous (Pd–Au) interactions were taken from [29]. The dynamical study in this work employs the (auxiliary) ADFT scheme, which is expected to provide additional isomers [30] different to those located by our semiempirical approach. This has been confirmed for Pd<sub>8</sub> cluster, which despite exhibiting identical lowest-energy configuration with both approaches, the energetical ordering for the rest of the low-lying isomers is overall distinct [31]. Likewise, additional isomer configurations are obtained through the DFT approach.

The dynamical process was studied through computer simulations based on the Born–Oppenheimer molecular dynamics (BOMD), employing ADFT energies and gradients within the NVT ensemble at T = 100 K to 400 K,

applying a Nosé-Hoover thermostat with a frequency of  $1500\text{ cm}^{-1}$  and a chain length of 3. The BOMD strategy has recently been utilized to obtain initial structures in ab initio global exploration of potential energy surfaces [32], as well as to understand the process of formation of ammonia, and is expected to be a valuable tool for providing microscopic insights in a number of potential chemical reactions [33]. The followed computational approach uses the linear combination of Gaussian-type orbital Kohn–Sham auxiliary density functional theory (LCGTO-KS-ADFT) as implemented in the deMon2k program [22]. The Perdew–Burke–Ernzerhof (PBE) functional [34] was utilized in combination with the Stuttgart–Dresden (SDD) basis set [35]. A quasi-relativistic effective core potential (QECP) was used to describe both Pd and Au atoms, which includes 18 and 19 valence electrons for Pd and Au atoms, respectively. The employed auxiliary basis set was GEN-A2\* in all calculations [36], and the total simulation time was at least 20 ps, with a time-step of 1 fs for each of the temperatures considered in this study.

To assess the effect of temperature on cluster structures, total energy dispersion profiles are examined at each temperature for both  $\text{Pd}_8$  and  $\text{Pd}_7\text{Au}_1$  clusters, and several representative structural motifs are collected from the simulation trajectories. This inspection of the structural evolution of clusters along the BOMD trajectory provides evidence on the structural changes underwent at each temperature and allows observing the existence of atomic diffusion. A careful examination of the recorded snapshots was carried out in this work. For the studied clusters, the caloric curves are presented as a criterion to perform a preliminary analysis of the corresponding thermodynamical behavior.

### 3 Results and discussion

Thermal stability is of paramount relevance in catalytic applications of metal clusters, and current theoretical studies disregard the importance of this thermodynamic variable on their structural properties. As a consequence, the physico-chemical predictions are performed on ideal equilibrium configuration clusters obtained from global exploration, empirical, or ab initio approaches. This is the current paradigm in cluster theoretical studies.

Figure 1 shows the total energy dispersion behavior of  $\text{Pd}_8$  cluster at temperatures 100 K to 400 K. As noted, the energy deviations oscillate around the average value of the total energy. Throughout all the BOMD trajectories, dispersion below and above the average energy is distributed equally, without depletion in partial time intervals for all the temperatures.

It is evident from this figure that as the temperature is raised, a steady increase in the energy dispersion occurs along the whole BOMD trajectory for temperatures 100 K

to 300 K. At 400 K, a dramatic change is presented by the energy dispersion from the average, thus manifesting the structural changes the cluster is undergoing. Analyzing the atomic configuration dynamical evolution of  $\text{Pd}_8$  atoms it is observed, in general, that the atomic configuration undergoes structural changes among a set of low-lying isomers, shown in Fig. 2. At 100 K, the cluster shows structural distortions but basically remains with the initial geometry. Two isomer configurations distinct to the initial are observed at 300 K. One of the predominant configurations at 300 K corresponds to a capped pentagonal bipyramid (see Panel 3).

Despite the drastic change in the energy dispersion profile, the atomic configuration analysis shows no evidence of atomic diffusion or bond-breaking at 400 K. Since in this work, the bond order has not been calculated, it has been assumed the existence of a bond when the distance between atoms is shorter than a cutoff distance. This is chosen to be about 10% longer than the Pd bulk bond distance,  $\langle d \rangle = 2.750\text{ \AA}$  [37]. The  $\text{Pd}_8$  cluster structure is severely distorted at this temperature, prevailing in the recorded BOMD trajectory that resembling the first isomer above the lowest-energy configuration for this cluster.

In Fig. 3, we show some configurations for  $\text{Pd}_7\text{Au}_1$  cluster, selected from the BOMD simulations carried out at various simulated temperatures. In all cases, the initial equilibrium configuration exhibits a bicapped octahedron geometry with  $D_{2d}$  symmetry. The gold and palladium capping atoms are initially located above and below the octahedron waist, formed by four Pd atoms. The selected snapshots shown for each temperature correspond to global and local minima in the cluster's PES, except that in panel 3 in which the AuPd dimer dissociates from the cluster at  $T=400\text{ K}$ . Some of the  $\text{Pd}_7\text{Au}_1$  configurations shown in this figure are reminiscent of structures present in different isomerization pathways previously described in anionic  $\text{Au}_{20}$  cluster by Cuny et al. [38].

In the first few time-steps of the BOMD simulation, a minimum energy configuration is reached at the PBE theory level. This low energy structure is located into a basin of the PES defined by the PBE functional for the  $\text{Pd}_7\text{Au}_1$  cluster. The PES of metal clusters is a multi-dimensional function of the atomic coordinates and spin variables, which is determined by the theoretical approach employed in the first principles calculations [39].

The analyzed 8-atom Pd–Au nanoalloy has one Au atom on the surface and, irrespective of the temperature, soon exhibits the tendency of this atom type to occupy low-coordinated sites. The geometry adopted in the equilibration period is caused by the maximization of the number Pd–Pd bonds, which is a consequence of the higher cohesive energy of palladium (3.89 eV/atom) compared to that of gold (3.81 eV/atom) [29]. Interestingly,  $\text{Pd}_7\text{Au}_1$  cluster fragmentation is observed at 400 K. The two fragments are one  $\text{Pd}_6$  octahedron and one Pd–Au dimer. At this temperature

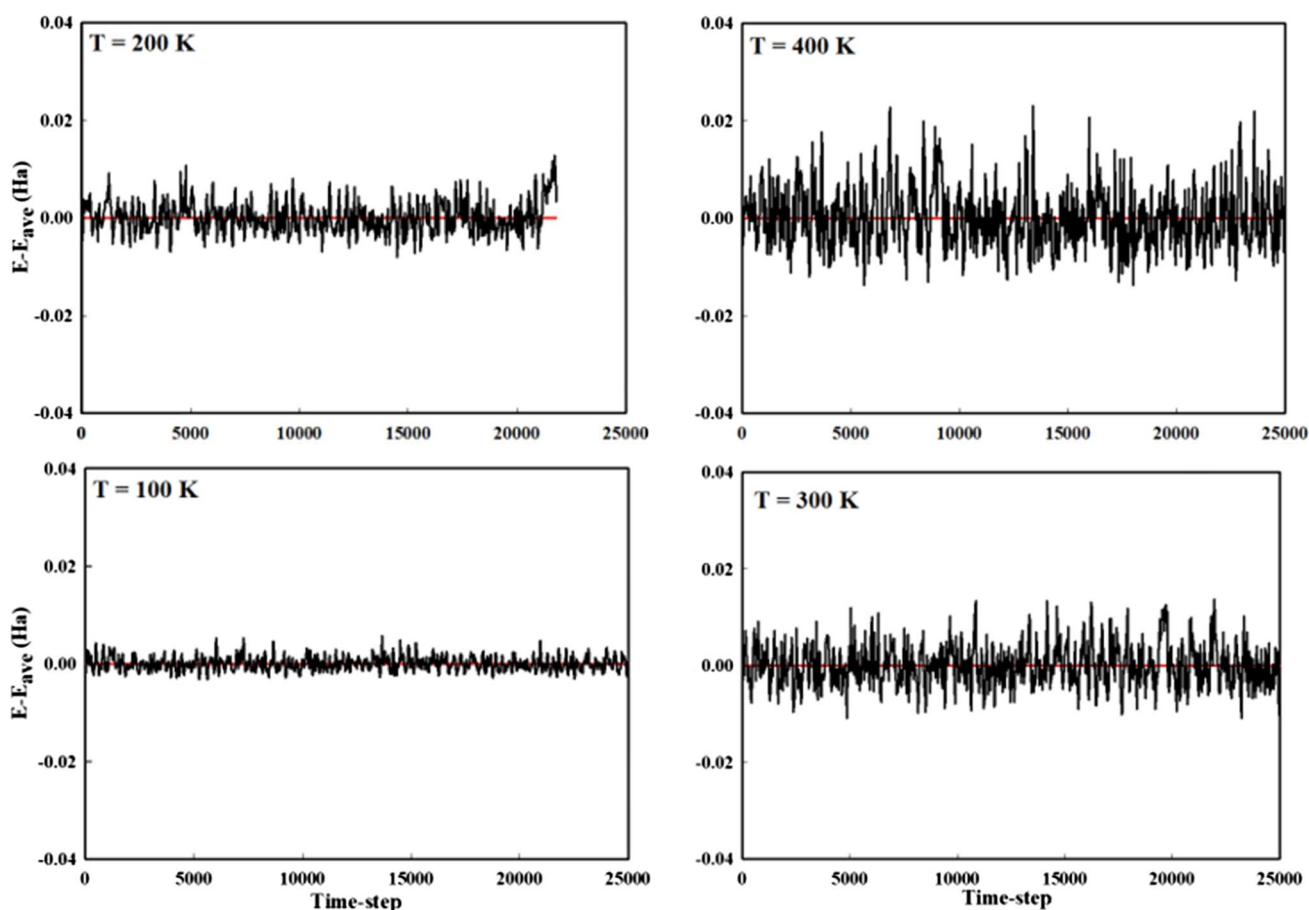


**Fig. 1** Plot of the total energy dispersion with respect to its average value for  $\text{Pd}_8$  cluster. The energy dispersion increases as the temperature is raised, observing a drastic change in energy dispersion at 400 K

(400 K), strong atomic oscillations, beyond the harmonic approximation, and a major contribution of the vibrational entropy are likely occurring. The latter plays a leading role in the phase transition phenomena. It is worth mentioning that high Au atom mobility is already observed in our simulations at 300 K, which might be an indication of liquid-like behavior around this temperature. At the Gupta level, the melting temperature of  $\text{Pd}_{55}$  has been estimated to be  $\sim 610$  K [40]. Clusters' melting point changes with both size and composition, thus making necessary further studies to determine the melting point at the DFT level, in particular for 8-atom Pd-based nanoalloys.

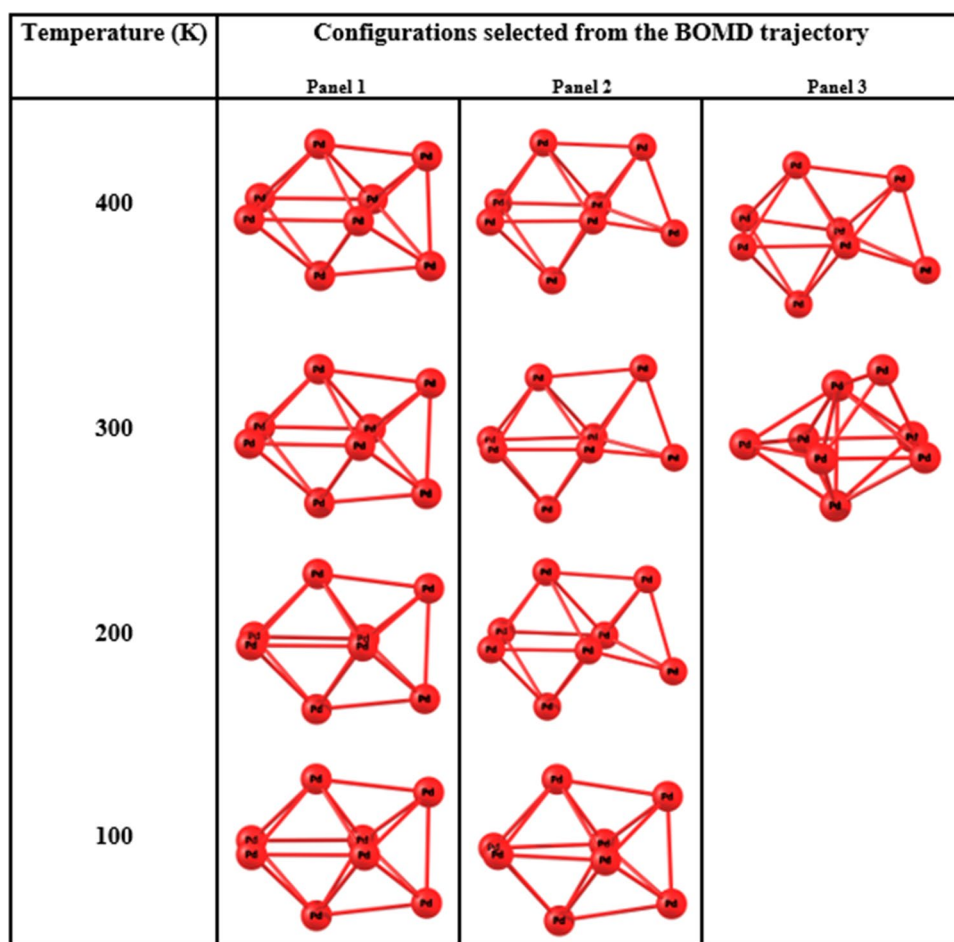
There are several molecular dynamics schemes that can be implemented to analyze the thermal stability of mono- and bimetallic clusters. The method employed in this study allows to obtain the total energy fluctuations at a given (fixed) finite temperature, while the number of atoms and cluster's volume are kept constant [41]. Computer simulations at a constant temperature result in the time evolution of the Cartesian coordinates of each of the atoms comprising the cluster. Thus, at each time-step, the structural and

energetic properties of clusters are fully determined, irrespective whether the simulation is based on classical or ab initio methods. The BOMD method utilized in this work has been successfully implemented for a number of systems [42–45].

Figure 4 shows the total energy deviation profiles obtained from the BOMD simulations for  $\text{Pd}_7\text{Au}_1$  cluster, at temperatures 100–400 K. The average total energy (red line) has been shifted to zero in order to better visualize the energy deviations from the average total energy value.

As the temperature increases, the magnitude of the total energy dispersion also increases. At 100 K, the energy dispersion oscillates below and above the average energy in two time periods. The first one proceeds during  $\sim 7$  ps, and thereafter, the second period occurs slightly above the average energy value. During the simulation, three different configurations are observed along the BOMD trajectory, the initial in which the Au atom coordination is maximum, and two others each detected on the above-mentioned periods. In the first time period, Au atom is displaced to a bridge site between two edge Pd atoms on the 7-Pd atom cluster (Panel

**Fig. 2** Pd<sub>8</sub> cluster configurations sampled from the BOMD trajectory obtained at the PBE theory level. Panel 1 shows the initial equilibrium configuration obtained from the empirical global optimization. Cluster configurations were sampled from ~20 ps or greater simulation time



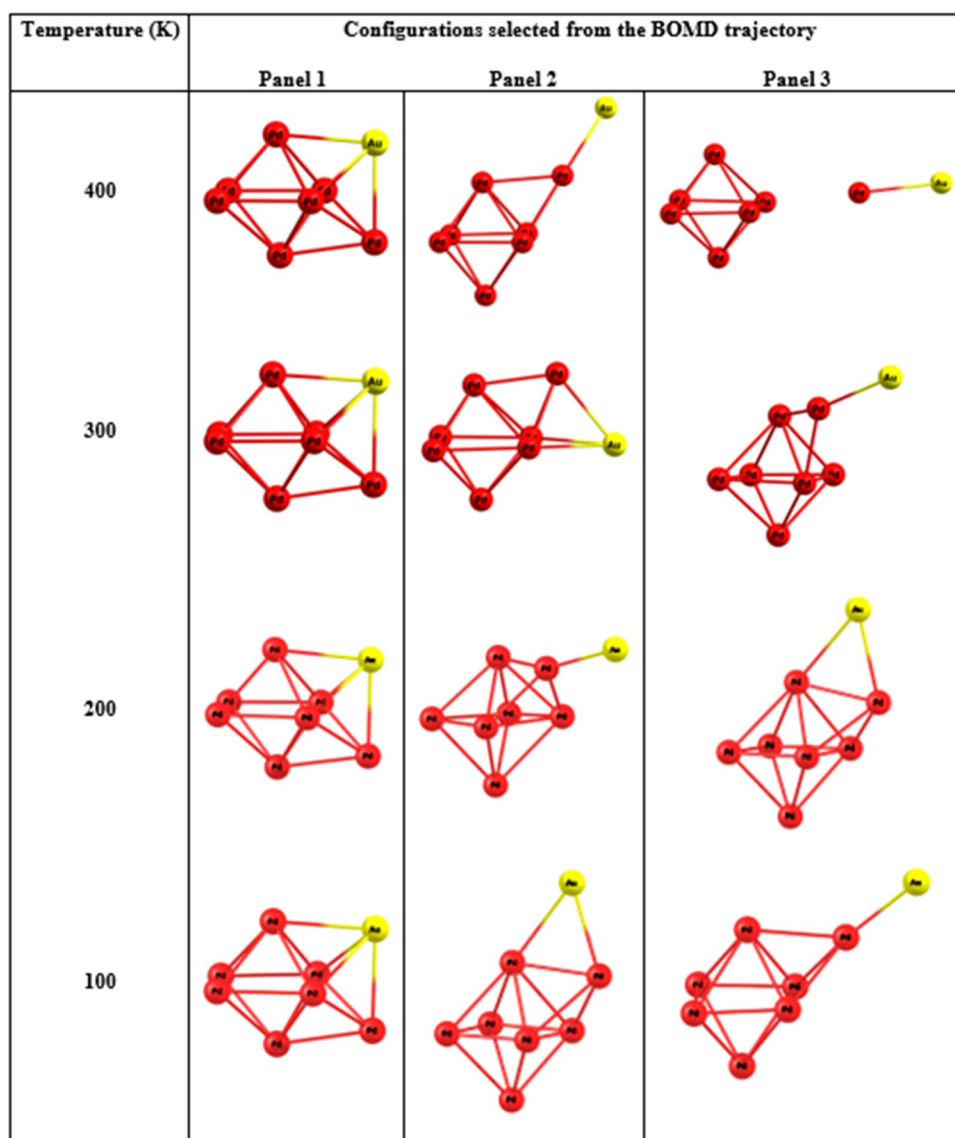
2 in Fig. 3 at 100 K), which is a (second isomer) capped octahedron according to both a thermal quenching study [46] and DFT minima search [47] performed to determine isomers of Pd<sub>7</sub> cluster. In the second time period, the Au atom is located on top of the capping Pd atom (Panel 3 in Fig. 3 at 100 K). This configuration has the lowest structural stability. In summary, the coordination of the Au atom is reduced at 100 K, with only three possible configuration to be detected. The lowest gold coordination configuration is observed longer in the BOMD trajectory.

The simulation at 200 K shows a slightly different behavior. The initial geometry soon disappears, as well as the configuration where the Au atom is located on a bridge position. Thus, the most likely configuration to be observed corresponds to that of the Au atom located on top of the Pd capping atom of the Pd<sub>7</sub> isomer. However, the dynamical behavior of the Pd<sub>7</sub>Au<sub>1</sub> cluster shows remarkable changes observed through the examination of the structural evolution of Pd<sub>7</sub>Au<sub>1</sub> cluster along the BOMD recorded trajectory. In Fig. 5, we show the structures illustrating an apparent Pd-Au dimer diffusion process.

In this figure, it is shown that the capping Pd atom together with the bonded Au atom move to hollow sites

of different triangular faces of the octahedron. This occurs by eventually crossing through the octahedron's edge. Our simulation shows that the Pd-Au dimer diffusion apparently begins to occur at this temperature, which can be interpreted as a premelting stage. The calculated activation energy barrier for the dimer passage from one triangular face to the neighbor face is about 0.011 Ha (~0.3 eV). A more detailed dynamical study is necessary in order to analyze whether this energy barrier corresponds to a self-diffusion energy barrier. Also, between 18 and 21 ps, the energy deviation describes an extreme. Kinetic energy in this time interval exhibits strong oscillations around a straight line, whereas the potential energy of cluster decreases. Thus, a basin of the PES is likely reached at this time interval. Similarly, at 300 K, it is more evident the presence of strong oscillations of the energy dispersion, as well as the existence of energy dispersion declinings below the average energy. Finally, at 400 K, the energy dispersion graph apparently shows, at the end of the simulation time, the cluster breakup through fragmentation in a 7-atom Pd cluster and the Pd-Au dimer, see Fig. 1 in Panel 3 at 400 K. Further studies are necessary to fully understand the kinetics of Pd<sub>7</sub>Au<sub>1</sub> cluster fragmentation at the DFT level. This is crucial to obtain reliable

**Fig. 3** Pd<sub>7</sub>Au<sub>1</sub> cluster configurations singled out from the BOMD trajectory obtained at the PBE theory level. Panel 1 shows the initial equilibrium configuration obtained from the empirical global optimization. In panel 2 and 3, we show typical configurations chosen from the BOMD trajectories, sampled from ~20 ps or greater simulation time



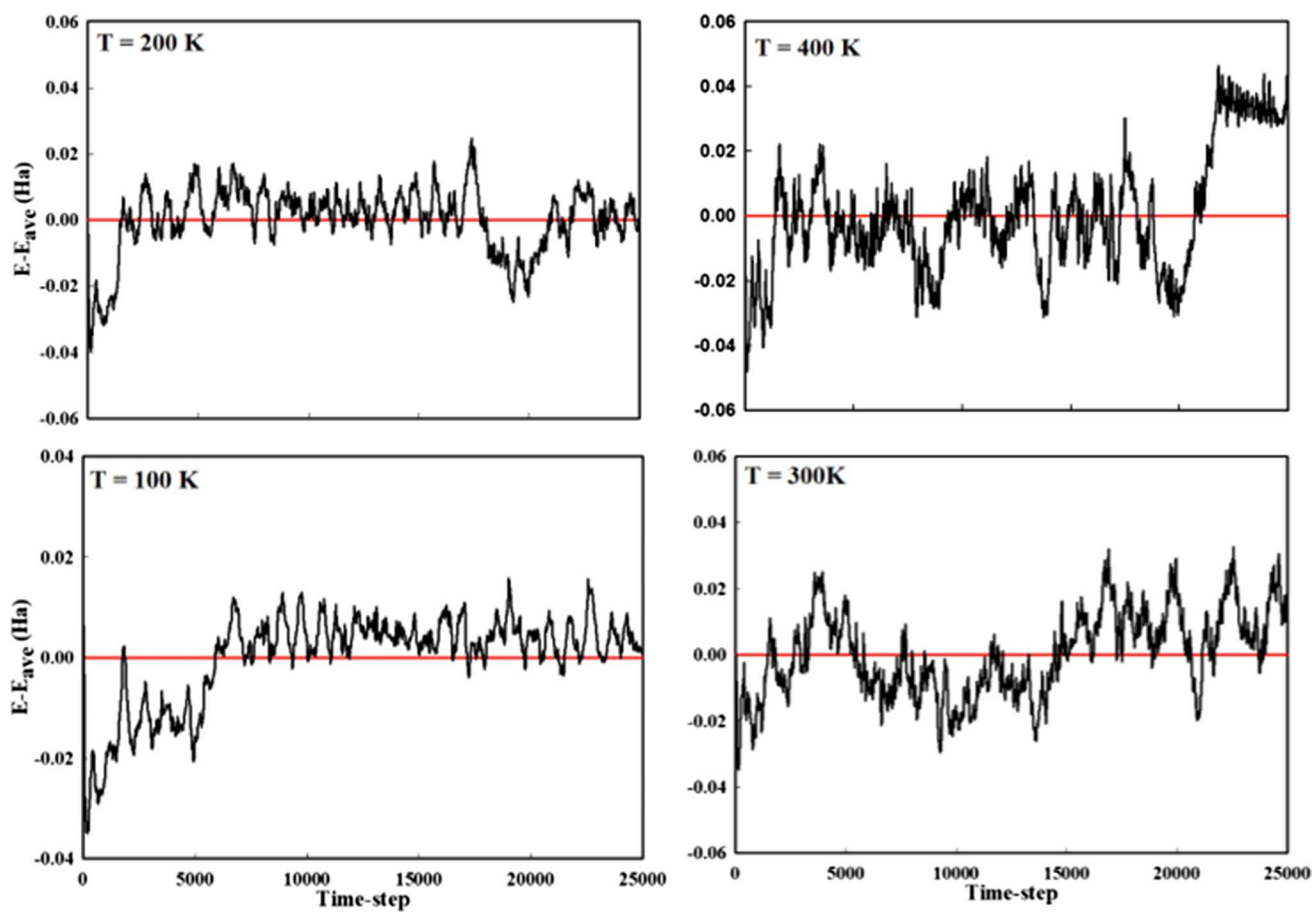
fragmentation predictions for this cluster, as well as for other sizes and compositions [14, 48].

With the aim of exploring the thermodynamical behavior of both Pd<sub>8</sub> and Pd<sub>7</sub>Au<sub>1</sub> clusters, the caloric curves are constructed utilizing the available information obtained from the BOMD simulation runs extracting from this the average total energy and temperature data. This criterion is used to estimate the temperature at which clusters undergo a phase transition. This criterion has been extensively used in several types of clusters, including metal clusters [49, 50]. As shown in Fig. 6 (a)–(b), the melting point of the Au-doped cluster is apparently reached between 200 and 300 K, while for Pd<sub>8</sub>, the phase transition is beyond the higher temperature utilized in this work simulations.

The linear behavior observed in (a) indicates that this cluster has not reached the melted state. In (b), the average total energy exhibits a discontinuity between 200 and

300 K. This behavior has been related to a sharp peak in the heat capacity indicating a phase transition. In this case, the caloric curve criterion suggests that the estimated melting temperature is about 250 K. Thus, this preliminary study shows that the effect of Au-doping on the palladium cluster is a declining in the melting temperature.

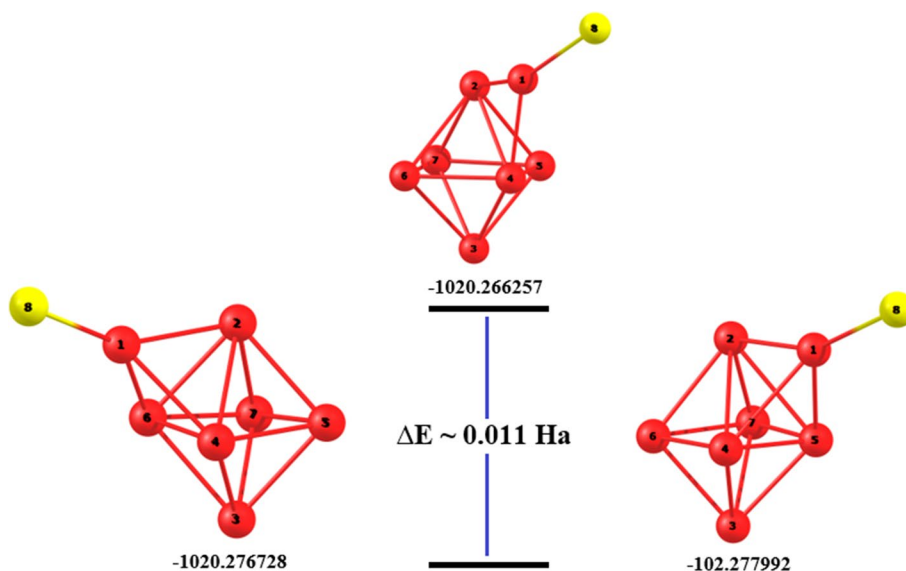
We must point out that more detailed studies are necessary to accurately estimate the melting temperature of Pd<sub>8</sub> cluster as well as additional schemes to confirm the melting transition. We must first confirm that the ergodic hypothesis holds in our simulations in order to determine reliable melting temperatures [51]. After this, the determination of the melting point can be implemented utilizing several of the common thermodynamical criteria. Additionally, longer simulation times are also necessary to obtain reliable predictions in both Pd<sub>8</sub> and Pd<sub>7</sub>Au<sub>1</sub> clusters, as well as a larger temperature range [52] and shorter temperature step around



**Fig. 4** Plot of the total energy deviation with respect to its average value for  $\text{Pd}_7\text{Au}_1$  cluster. The energy dispersion increases as the temperature is raised and strong oscillations are observed above 300 K.

Positive (negative) deviations are related to lower (higher) relative stability regarding to average energy configurations

**Fig. 5** Pd-Au dimer dynamical process observed at 200 K between 18 and 21 ps. Pd atoms are numbered for better visualize the dimer passage from one triangular face to the neighbor one in the octahedron. Cluster total energy is given below each structure (in Ha). It is important to note that the energy difference shown in the structure of the cluster, left and right in this figure, is less than the typical experimental error (1 kcal/mol or 0.0016 Ha)



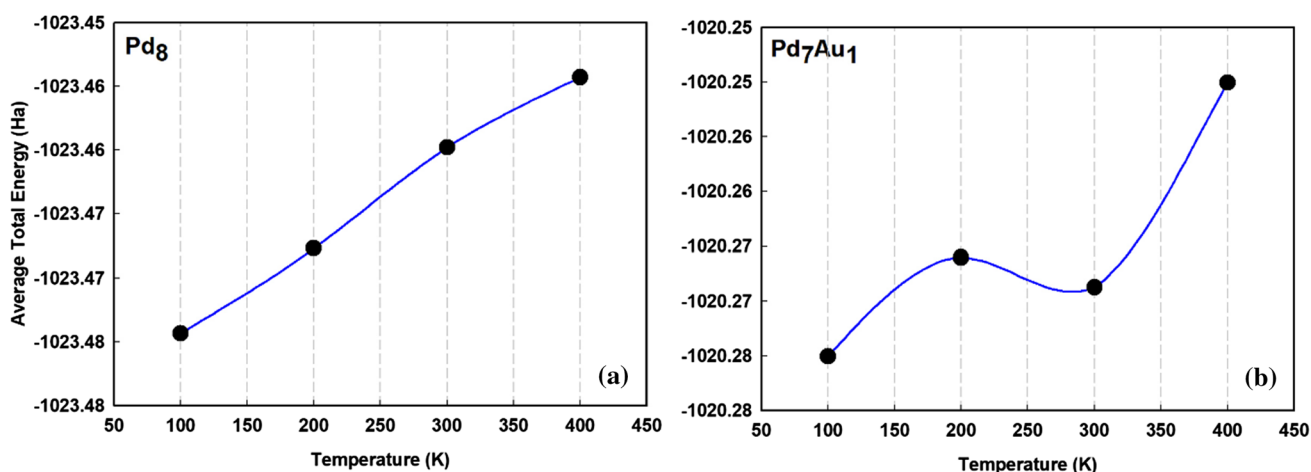


**Fig. 6** Plot of the average total energy as a function of temperature for **a** Pd<sub>8</sub> and **b** Pd<sub>7</sub>Au<sub>1</sub> clusters

the phase transition temperature. These studies are feasible with the ADFT BOMD methodology utilized in this work.

## 4 Conclusions

In this work, we have utilized a combined strategy to study the thermal effects on the structure of Pd<sub>8</sub> and Pd<sub>7</sub>Au<sub>1</sub> clusters. This combined approach, based on semiempirical global explorations and DFT BOMD simulations as implemented in deMon2k, speeds up both the static and dynamic calculations and facilitates the identification of the different regions of the BO potential energy surface at low temperatures. Likewise, it allows analyzing the effect of single-atom doping on the structure of pure clusters at different thermodynamic states relatively quickly. Our simulation results have shown the higher thermal stability of pure Pd<sub>8</sub> cluster compared to that of the Pd<sub>7</sub>Au<sub>1</sub>. Irrespective of the temperature, the single Au atom prefers low coordination sites on the palladium cluster structure. Our computer simulations also demonstrated that bimetallic cluster fragmentation occurs through the dissociation of the Pd-Au dimer and the octahedra Pd<sub>6</sub> cluster. A rough estimation of the melting temperature has been obtained for Pd<sub>7</sub>Au<sub>1</sub> cluster of ~250 K. However, additional studies to accurately determine the melting point of both Pd<sub>7</sub>Au<sub>1</sub> and Pd<sub>8</sub> clusters are still necessary. These studies are feasible using the present ADFT BOMD methodology to perform longer MD runs, on the order of nanoseconds, and utilizing smaller temperature intervals to explore the phase transition region adequately.

**Acknowledgements** The authors are grateful to Conacyt for funding project No. A1-S-39326. AL-V also acknowledges Conacyt for the award of a Ph.D. scholarship.

**Funding** APA is grateful to Consejo Nacional de Ciencia y Tecnología for funding project No. A1-S-39326 AL-V acknowledges Consejo Nacional de Tecnología for the award of a Ph.D. scholarship.

**Data availability and material** Data are provided in supplementary zip files including the BOMD trajectories for both Pd<sub>8</sub> and Pd<sub>7</sub>Au<sub>1</sub> clusters.

## Declarations

**Conflict of interest** The authors declare no conflict of interest.

## References

1. Seminario JM, Agapito LA, Yan L, Balbuena PB (2005) Density functional theory study of adsorption of OOH on Pt-based bimetallic clusters alloyed with Cr Co, and Ni. *Chem Phys Lett* 410:275–281
2. Larios-Rodríguez EA, Castellón-Barraza FF, Herrera-Urbina R, Santiago U, Posada-Amarillas A (2017) Synthesis of Au@Pd-shell nanoparticles by a green chemistry method and characterization by HAADFSTEM imaging. *J Clust Sci* 28:2075–2086
3. Cristoforetti G, Pitzalis E, Spiniello R, Ishak R, Muniz-Miranda M (2011) Production of palladium nanoparticles by pulsed laser ablation in water and their characterization. *J Phys Chem C* 115:5073–5083
4. Thakkar KN, Mhatre SS, Parikh RY (2010) Biological synthesis of metallic nanoparticles. *Nanomedicine: NBM* 6:257–262
5. Heck RF, Nolley JP (1972) Palladium-catalyzed vinylic hydrogen substitution reactions with aryl, benzyl, and styryl halides. *J Org Chem* 37:2320–2322
6. Mizoroki T, Mori K, Ozaki A (1971) Arylation of olefin with aryl iodide catalyzed by palladium. *Bull Chem Soc Jap* 44:581
7. Miyaura N, Yamada K, Suzuki A (1979) A new stereospecific cross-coupling by the palladium-catalyzed reaction of 1-alkenylboranes with 1-alkenyl or 1-alkynyl halides. *Tetrahedron Lett* 20:3437–3440
8. Miyaura N, Suzuki A (1995) Palladium-catalyzed cross-coupling reactions of organoboron compounds. *Chem Rev* 95:2457–2483

9. Yin L, Liebscher J (2007) Carbon–carbon coupling reactions catalyzed by heterogeneous palladium catalysts. *Chem Rev* 107:133–173
10. Roglans A, Pla-Quintana A, Moreno-Mañas M (2006) Diazonium salts as substrates in palladium-catalyzed cross-coupling. *Chem Rev* 106:4622–4643
11. Tseng JY, Cheng HT (2020) Catalytic ethylene oxidation by Cu–Au core–shell nanoclusters: a computational study. *Theor Chem Acc* 139:57
12. Saxena R, Saravindakshan SU, Qureshi M, De M (2020) Supported palladium nanoclusters: Morphological modification towards enhancement of catalytic performance using surfactant-assisted metal deposition. *Appl Nanosci* 10:1793–1809
13. Klaja O, Szczygieł J, Trawczyński J, Szyja BM (2017) The CO<sub>2</sub> dissociation mechanism on the small copper clusters—The influence of geometry. *Theor Chem Acc* 136:98
14. Gálvez-González LE, Juárez-Sánchez JO, Pacheco-Contreras R, IGarzón IL, Paz-Borbón LO, Posada-Amarillas A (2018) CO<sub>2</sub> adsorption on gas-phase Cu<sub>4–x</sub>Pt<sub>x</sub> (x = 0–4) clusters: A DFT study. *Phys Chem Chem Phys* 20: 17071–17080
15. Gálvez-González LE, Alonso JA, Paz-Borbón LO, Posada-Amarillas A (2019) H<sub>2</sub> adsorption on Cu<sub>4–x</sub>M<sub>x</sub> (M = Au, Pt; x = 0–4) clusters: Similarities and differences as predicted by density functional theory. *J Phys Chem C* 123: 30768–30780
16. Khirsariya P, Mewada RK (2013) Single step oxidation of methane to methanol—Towards better understanding. *Procedia Eng* 51:409–415
17. Petrov AW, Ferri D, Krumeich F, Nachtegaal M, van Bokhoven JA, Kröcher O (2018) Stable complete methane oxidation over palladium based zeolite catalysts. *Nature Commun* 9:2545
18. Cheng D, Atanasov IS, Hou M (2011) Influence of the environment on equilibrium properties of Au–Pd clusters. *Eur Phys J D* 64:37–44
19. Cristoforetti G, Pitzalis E, Spiniello R (2011) Production of palladium nanoparticles by pulsed laser ablation in water and their characterization. *J Phys Chem C* 115:5073–5083
20. Ning X, Zhan L, Wang H, Yu H, Peng F (2018) Deactivation and regeneration of in situ formed bismuth-promoted platinum catalyst for the selective oxidation of glycerol to dihydroxyacetone. *New J Chem* 42:18837–18843
21. Luo C, Zhou C, Wu J, Kumar TJD, Balakrishnan N, Forrey RC, Cheng H (2007) First principles study of small palladium cluster growth and isomerization. *Int J Quantum Chem* 107:1632–1641
22. Köster A, Geudtner G, Alvarez-Ibarra A, Calaminici P, Casida M, Carmona-Espindola J, Dominguez V, Flores-Moreno R, Gamboa G, Goursot A, Heine T, Ipatov A, de la Lande A, Janetzko F, del Campo J, Mejia-Rodriguez D, Reveles JU, Vasquez-Perez J, Vela A, Zuniga-Gutierrez B, Salahub DR (2018) deMon2k, version 5. The deMon developers, Cinvestav, México City
23. Pacheco-Contreras R, Juárez-Sánchez JO, Dessens-Félix M, Aguilera-Granja F, Fortunelli A, Posada-Amarillas A (2018) Empirical-potential global minima and DFT local minima of trimetallic Ag<sub>l</sub>Au<sub>m</sub>Pt<sub>n</sub> (l + m + n = 13, 19, 33, 38) clusters. *Comp Mater Sci* 141:30–40
24. Wales DJ (1997) Doye JPK (1997) Global optimization by basin-hopping and the lowest energy structures of Lennard-Jones clusters containing up to 110 atoms. *J Phys Chem A* 101:5111–5116
25. Posada-Amarillas A, Garzón IL (1996) Microstructural analysis of simulated liquid and amorphous Ni. *Phys Rev B* 53:8363–8368
26. Borbón-González DJ, Fortunelli A, Barcaro G, Sementa L, Johnston RL, Posada-Amarillas A (2013) Global minimum Pt<sub>13</sub>M<sub>20</sub> (M = Ag, Au, Cu, Pd) dodecahedral core-shell clusters. *J Phys Chem A* 117:14261–14266
27. Guerrero-Jordan J, Cabellos JL, Johnston RL, Posada-Amarillas A (2018) Theoretical investigation of the structures of unsupported 38-atom CuPt clusters. *Eur Phys J B* 91:123
28. Cleri F, Rosato V (1993) Tight-binding potentials for transition metals and alloys. *Phys Rev B* 48:22–33
29. Ismail R, Johnston RL (2010) Investigation of the structures and chemical ordering of small Pd–Au clusters as a function of composition and potential parameterisation. *Phys Chem Chem Phys* 12:8607–8619
30. Heard CJ, Johnston RL, Schön JC (2015) Energy landscape exploration of sub-nanometre copper–silver clusters. *ChemPhysChem* 16:1461–1469
31. Luna-Valenzuela A, Alonso JA, Cabellos, JL, Posada-Amarillas, A (2021) Effects of van der Waals interactions on the structure and stability of Cu<sub>8–x</sub>Pd<sub>x</sub> (x = 0, 4, 8) cluster isomers. *Mater. Today Commun.* 26:102024
32. López-Sosa L, Cruz-Martínez H, Solorza-Feria O, Calaminici P (2019) Nickel and copper doped palladium clusters from a first-principles perspective. *Int J Quantum Chem* 119:e26013
33. Yamijala SSRKC, Nava G, Ali ZA, Beretta D, Wong BM (2020) Harnessing plasma environments for ammonia catalysis: Mechanistic insights from experiments and large-scale *ab initio* molecular dynamics. *J Phys Chem Lett* 11:10469–10475
34. Perdew JP, Burke K, Ernzerhof M (1996) Generalized gradient approximation made simple. *Phys Rev Lett* 77:3865–3868
35. Dolg M, Cao X (2012) Relativistic pseudopotentials: Their development and scope of applications. *Chem Rev* 112:403–480
36. Calaminici P, Janetzko F, Köster AM, Mejia-Olvera R, Zuniga-Gutierrez B (2007) Density functional theory optimized basis sets for gradient corrected functionals: 3d transition metal systems. *J Chem Phys* 126:044108
37. Krüger S, Vent S, Nörtemann F, Stauffer M, Rösch N (2001) The average bond length in Pd clusters Pd<sub>n</sub>, n = 4–309: A density-functional case study on the scaling of cluster properties. *J Chem Phys* 115:2082–2087
38. Cuny J, Tarrat N, Spiegelman F, Huguenot A, Rapacioli M (2018) Density-functional tight-binding approach for metal clusters, nanoparticles, surfaces and bulk: application to silver and gold. *J. Phys.: Condens. Matter* 30:303001
39. Ferrando R (2013) In: Mariscal MM, Oviedo OA, Marcos-Leiva EP (ed) *Metal Clusters and Nanoalloys: From Modeling to Applications*, Springer, New York
40. Cheng D, Wang W (2012) Tailoring of Pd–Pt bimetallic clusters with high stability for oxygen reduction reaction. *Nanoscale* 4:2408–2415
41. Andersen HC (1980) Molecular dynamics simulations at constant pressure and/or temperature. *J Chem Phys* 72:2384–2393
42. Gamboa GU, Calaminici P, Geudtner G, Köster AM (2008) How important are temperature effects for cluster polarizabilities? *J Phys Chem A* 112:11969–11971
43. Vásquez-Pérez JM, Martínez GUG, Köster AM, Calaminici P (2009) The discovery of unexpected isomers in sodium heptamers by Born–Oppenheimer molecular dynamics. *J Chem Phys* 131:124126
44. Alvarez-Ibarra A, Calaminici P, Goursot A, Gómez-Castro CZ, Grande-Aztatzi R, Mineva T, Salahub DR, Vásquez-Pérez JM, Vela A, Zuniga-Gutierrez B, Köster AM (2015) Chapter 7—First principles computational biochemistry with deMon2k In: Ul-Haq Z, Madura, JD (ed) *Frontiers in Computational Chemistry*; Bentham Science Publishers: Sharjah, UAE.
45. de la Lande A, Alvarez-Ibarra A, Hasnaoui K, Cailliez F, Wu X, Mineva T, Cuny J, Calaminici P, López-Sosa L, Geudtner G, Navizet I, Garcia Iriepa C, Salahub DR, Köster AM (2019) Molecular simulations with in-deMon2k QM/MM, a tutorial-review. *Molecules* 24:1653
46. Karabacak M, Özçelik S, Güvenç ZB (2004) Dynamics of phase changes and melting of Pd<sub>7</sub> clusters. *Acta Phys Slovaca* 54:233–243

47. Zanti G, Peeters D (2010) DFT study of bimetallic palladium-gold clusters Pd<sub>n</sub>Au<sub>m</sub> of low nuclearities ( $n + m \leq 14$ ). *J Phys Chem A* 114:10345–10356
48. Passananti M, Zapadinsky E, Zanca T, Kangasluoma J, Myllys N, Rissanen MP, Kurtén T, Ehn M, Attoui M, Vehkamäki H (2019) How well can we predict cluster fragmentation inside a mass spectrometer? *Chem Comm* 55:5946–5949
49. Oderji HY, Ding H (2011) Determination of melting mechanism of Pd<sub>24</sub>Pt<sub>14</sub> nanoalloy by multiple histogram method via molecular dynamics simulations. *Chem Phys* 388:23–30
50. Ferrando R, Jellinek J, Johnston RL (2008) Nanoalloys: from theory to applications of alloy clusters and nanoparticles. *Chem Rev* 108:845–910
51. Hannemann A, Schön JC, Jansen M, Sibani P (2005) Non-equilibrium dynamics in amorphous Si<sub>3</sub>B<sub>3</sub>N<sub>7</sub>. *J Phys Chem B* 109:11770–11776
52. Vázquez-Pérez JM, Calaminici P, Köster AM (2013) Heat capacities from Born-Oppenheimer molecular dynamics simulations: Al<sub>27</sub><sup>+</sup> and Al<sub>28</sub><sup>+</sup>. *Comp Theor Chem* 1021:229–232

**Publisher's Note** Springer Nature remains neutral with regard to jurisdictional claims in published maps and institutional affiliations.